

Research on the civil aero-engine modeling method oriented to control law design

Shuai Liu

Civil Aviation University of China

Ming Zhang

Civil Aviation University of China

Wei Wang (✉ 918817735@qq.com)

Civil Aviation University of China

Jie Bai

Civil Aviation University of China

ShiJie Dai

Hebei University of Technology

Research Article

Keywords: Aero engine, Modeling, Control standard model, Control law

Posted Date: November 9th, 2021

DOI: <https://doi.org/10.21203/rs.3.rs-1029183/v1>

License: © ⓘ This work is licensed under a Creative Commons Attribution 4.0 International License.

[Read Full License](#)

Research on the civil aero-engine modeling method oriented to control law design

LIU Shuai¹ ZHANG Ming² WANG Wei¹ BAI Jie¹ DAI ShiJie³

(1. Key Laboratory for Civil Airworthiness Certification Technology, Civil Aviation University of China; Tianjin 300300, China;

2. Sino-European Institute of Aviation Engineering, Civil Aviation University of China; Tianjin 300300, China;

3. School of Mechanical Engineering, Hebei University of Technology, Tianjin 300130, China)

Abstract: The non-linear aero-thermal model of civil aero-engine established by the component method has the characteristics of complex structure and strong coupling of parameters, which is difficult to directly use in the design of control law. Aiming at the problem that civil aero-engine control law design is difficult, heavy workload, and can only be used for nominal point linearization model, a civil aero-engine modeling method oriented to control law design is proposed.

Simplify the structure according to the aero-engine control function, and use rotor dynamics modeling and combustion reaction dynamics modeling to establish aero-engine control standard model in differential form, which establishes the corresponding relationship of the parameters required for the control of the aero-engine full envelope. With this control standard model, the nonlinear control method can be directly used in the design of the aero-engine control law, which reduces the workload and difficulty of the control law design to certain extent. The control standard model is established by taking DGEN380 aero-engine as an example, whose accuracy is verified through experiments, and an example of the control law design is given. The civil aviation engine modeling method oriented to control law design has achieved the expected goal.

Key words: Aero-engine; Modeling; Control standard model; Control law

Corresponding author : Dr. Wang Wei

1. Introduction

The aero-engine control system is used to realize the thrust response of the aero-engine and ensure that the aero-engine is in a safe state, and is an important system to exert the performance of the aero-engine and ensure the safety of the aero-engine. The aero-engine control system takes its control law as the core. The most critical part in the aero-engine control law design process is the modeling of aero-engine, which takes more than 60% of the controller design time.^[1]

The component method is recognized in the industry as a modeling method in the controller design stage. The non-linear aero-thermal model of aero-engine is obtained through component method modeling, which has complex structure, severe coupling of various thermal parameters, and is difficult to solve, so it cannot be directly used for control law design^[2-4]; It needs to be linearized at the nominal point to obtain a linear model in the neighborhood of the nominal point, so as to design the local control algorithm and the global control algorithm.

The component method modeling comes from the aero-engine performance analysis, and its model is different from the model required for the design of the civil aero-engine controller. The earliest component method modeling idea was proposed by Otto and Taylor in the 1950s, which solved the problem of performance analysis in aero-engine design^[5]. The development of the component method has gone through the stages of SMOTE code, GENENG code, and DYNGEN code. The National Aeronautics and Space Administration (NASA) obtained the high-fidelity simulation code CMAPSS on the basis of the DYNGEN code^[6-9] at the beginning of this century. The development process of aero-engine modeling based on the component method is shown in Figure 1.

The component method modeling forms a complete machine-level nonlinear aero-thermal model through joint working equations with the basis of the establishment of the aero-thermal relationship of each component of the aero-engine, which involves many parameters and can extract the aero-thermal parameters of each station in real time. However, large amount of parameters has become "barriers" to the design of civil aero-engine controllers. Civil aero-engine controls engine thrust and restricts key parameters by adjusting fuel flow, parameters required for aero-engine control include low-pressure rotor speed that characterizes thrust, high-pressure rotor speed that is safely restricted, and turbine temperature. In other words, not all parameters of each station are required for the control law design. So

the model established by the component method differs from the model required for civil aviation engine control law design. The model established by the component method is strongly nonlinear, and includes numerous parameters which are mutual coupling, which directly increases the workload and difficulty of control law design, moreover, which affects the architectural form of the civil aero-engine control system, that is, local control algorithm with global control algorithm scheduling nominal point. This architectural form cause that many advanced control algorithms (such as sliding mode variable structure, model prediction) only acts on one nominal point of linear model, and cannot reflect the advantages of nonlinear control method.

Therefore, aiming at control law design, this article regards aero-engine as a power system rather than a collection of components, and establishes general civil aero-engine model which mainly focuses on the necessary parameters required for control law design, has the form of $dx/dt=f(x)+g(x)u$ and can be directly used in the of nonlinear control law design, so as to obtain a civil aero-engine modeling method oriented to the design of control law. The model established by this method is named as aero-engine control standard model.

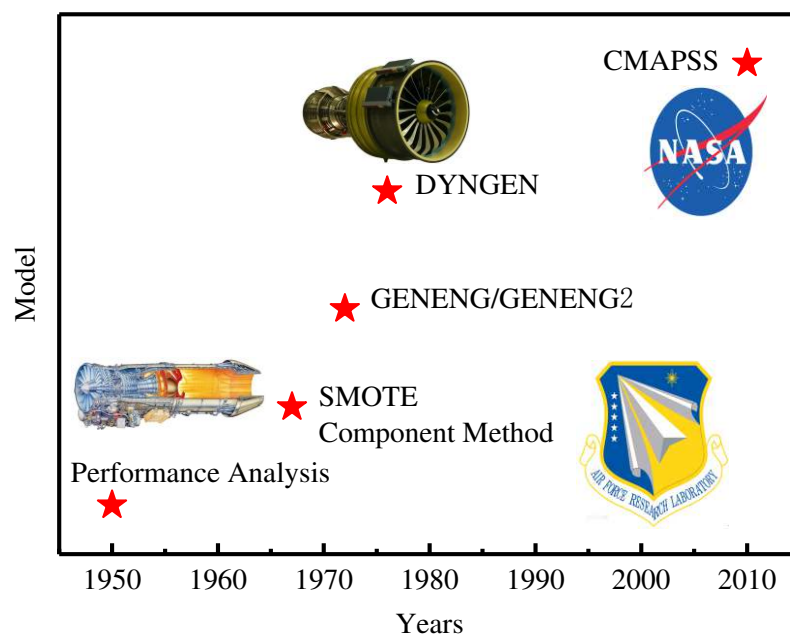


Figure1 The development process of component method modeling

2.civil aero-engine modeling method oriented to control law design

2.1 Analysis of Aero-Engine Control Function

The main function of civil aero-engine control is to calculate the fuel flow of the aero-engine based on the throttle lever angle, flight conditions and other parameters to ensure the thrust level of the aero-engine. Among them, the aero-engine control ensuring the thrust level has three meanings: (1) maintain the specified thrust value in the steady state so that it does not change with disturbances, (2) ensure that the thrust changes smoothly within the required time in the transition state, (3) ensure that the limit parameters of the aero-engine do not exceed the limit.

It can be known from the civil aero-engine control function that thrust, thrust change rate, limit protection parameters and fuel flow are the necessary parameters for civil aero-engine control law during the control process.

2.2 Aero-engine modeling analysis

The main task of aero-engine control is to control thrust. Turbofan engines are representative of civil aero-engines. The thrust of the turbofan engine is mainly produced by the fan compressed air, which produces more than 80% of the total thrust, and the other part is produced by the expansion and acceleration of high temperature and high pressure gas in the turbine and nozzle. The fan is driven by a turbine, and the rotation of the turbine is derived from the high-temperature and high-pressure gas produced by the compressor and combustion chamber. The high-temperature and high-pressure gas not only makes the turbine rotate with fan to generate thrust, but also expands and accelerates in the turbine to generate thrust. Therefore, high-temperature and high-pressure gas is the source of thrust for aero-engines. The established aero-engine model is to describe the mapping relationship between high temperature and high pressure gas and aero-engine thrust.

The low-pressure rotor speed is generally chosen to characterize the thrust of the civil aero-engine. High-temperature and high-pressure of gas originate from the supercharging process and the combustion process. The change of compressor power can reflect the supercharging process of the air flow, and the temperature change in

the combustion chamber can reflect the combustion process of gas and fuel. The combustion reaction kinetic equation is selected to simulate the mixed combustion of high-pressure airflow and fuel, and the temperature change of the combustion chamber is output; The rotor differential term of the rotor dynamics equation is selected to simulate the change of the rotor speed, that is, the thrust change. The compressor power term of the rotor dynamics equation simulates the boosting process of the air flow, and the turbine power term can simulate the expansion and acceleration process of high temperature and high pressure gas, and the combustion reaction dynamics equation is coupled with the rotor dynamics equation through the outlet temperature parameter of the combustion chamber in the turbine power term.

The high-temperature and high-pressure gas is supercharged by the rotation of the rotor and the temperature increases by fuel combustion, but the reason for maintaining the rotation of the rotor is that the fuel converts chemical energy into internal energy of the gas that works on the turbine through combustion. The aero engine model designed for the control law needs to describe the mapping relationship between combustion chamber fuel and low-pressure rotor speed.

The general civil turbofan engine structure diagram is shown in Figure 2. The fan module in the figure includes a booster, which is omitted in the figure; the dotted line-number in the figure is the aero-engine position information, which is placed at the aerodynamic parameter corner to indicate the aerodynamic parameter position. In order to enhance the modeling versatility to meet the modeling requirements of the geared turbofan engine, a gear reducer is installed between the low-pressure rotor and the fan. For turbofan engines without gear reducers, set the reduction ratio to 1. The aero-engine in the picture has two shafts, a high pressure and a low pressure, which are aerodynamically connected. The area of the tail nozzle of the aero-engine is not adjustable. As shown in the figure, the fuel is represented by the fuel flow rate W_f . When the fuel enters the combustion chamber of the aero engine, the chemical energy of the fuel is converted into gas internal energy, and then the temperature before the high-pressure turbine T_4 rises, and the high-pressure turbine changes accordingly, thereby affecting the high-pressure shaft speed N_2 , next, high temperature and high pressure gas expands in the high-pressure turbine, and enters the low-pressure turbine. Because the temperature before the low-pressure turbine T_{45} is aerodynamically connected with T_4 , the change of T_{45} causes the low-pressure turbine to change accordingly, thereby affecting the low-pressure shaft speed N_1 . The rotor dynamics

equations of the high-pressure shaft and the low-pressure shaft are established respectively, which are related through the aerodynamic relationship $T_4 = \Phi(T_{45})$, and T_{45} is obtained through the combustion reaction kinetic equation.

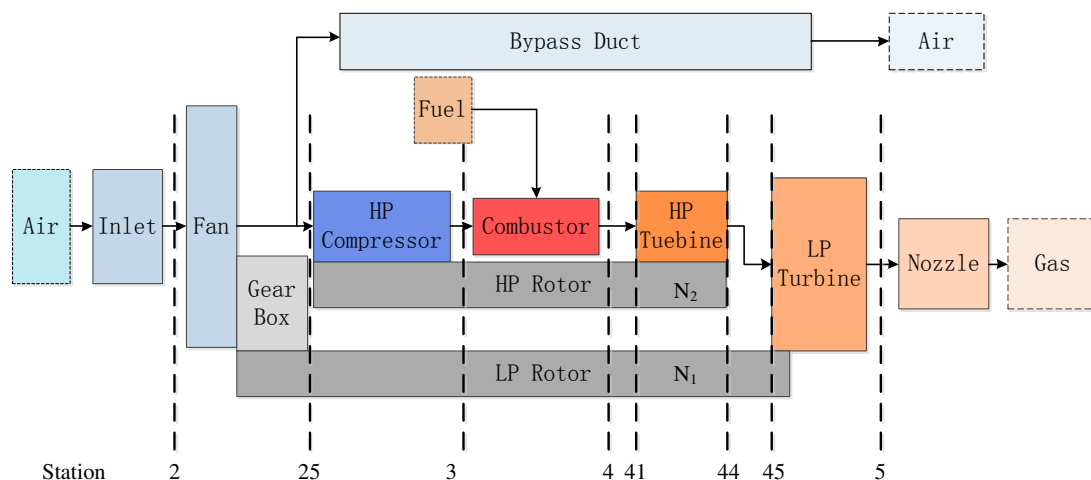


Figure2 Civil aero-engine structure diagram

2.3 Simplification assumptions in modeling

This article only analyzes the idle state, climb state, cruise state and the transition process between these states of aero-engine, therefore, the assumption condition ignores the aero engine start and stop process. Considering the mixed combustion process of the fuel and high-pressure air flow in the modeling, the combustion reaction kinetic equation is used to describe the combustion process. The reaction mechanism of fuel combustion is involved in the combustion reaction kinetic modeling, most civil aero-engines use Jet A aviation kerosene as fuel, so it is assumed as the aero-engine fuel in the modeling. The compressor efficiency, turbine efficiency, low-pressure rotor mechanical efficiency, and high-pressure rotor mechanical efficiency are treated as time variables instead of constant value parameters in the modeling process, and fan/compressor efficiency, turbine efficiency, low-pressure rotor mechanical efficiency, and high-pressure rotor mechanical efficiency changing with the speed of the high-pressure/low-pressure rotor (that is, the state of the compressor and the turbine) is considered. Besides, the specific heat capacity parameter is also treated as a variable in the modeling process.

2.4 Aero-engine modeling oriented to control law design

According to the analysis of aero-engine modeling, the rotor rotation process and combustion process are the core of aero-engine modeling. The rotor dynamics model and the combustion reaction dynamics model are established respectively.

(1) Rotor dynamics modeling

The rotor of an aero-engine connects the compressor (fan) and the turbine. The rotor dynamics equation establishes the relationship between the rotor speed change, the compressor power (fan power) and the turbine power. The rotor dynamics equation is as formula (1).

$$\frac{d\omega}{dt} = \frac{1}{J\omega} \cdot (P_t - P_c) \quad (1)$$

Where: t is the time; ω is the angular velocity of the rotor; J is the moment of inertia of the rotor; P_t is the output power of the turbine, P_c is the consumption power of the compressor. Convert the rotor angular velocity in equation (1) into the rotor speed N , then the equation (2) is obtained as follows:

$$\left(\frac{\pi}{30}\right)^2 JN \frac{dN}{dt} = P_t - P_c \quad (2)$$

The left side of equation (2) contains all variables related to the rotor, the rotor's moment of inertia, rotor speed, and changes of rotor speed; the right side is the difference between turbine power and compressor power, that is, the remaining power of the rotor. Equation (2) shows that the product of all variables of the rotor is proportional to the remaining power of the rotor. The rotor dynamics equations of the high-pressure rotor and low-pressure rotor are established respectively according to their respective characteristics on the basis of equation (2), as shown in equations (3) and (4), where the subscript L represents low pressure and H represents high pressure.

$$\left(\frac{\pi}{30}\right)^2 J_H N_H \frac{dN_H}{dt} = P_{HPT} - P_{HPC} \quad (3)$$

$$\left(\frac{\pi}{30}\right)^2 J_L N_L \frac{dN_L}{dt} = P_{LPT} - P_{FAN} \quad (4)$$

According to the aero-thermal relationship, formulas (3) and (4) are simplified to obtain formulas (5) and (6) as follows:

$$K_{J1} \frac{d \ln \bar{N}_1}{dt} = \left[\frac{c_p \eta_T^* \eta_L}{n_{cor,LPT}^2} \left(1 - \frac{1}{e_{LT}}\right) (q_{25} + W_f) - \frac{1}{n_{cor,FAN}^2} \frac{c_p (e_F - 1) q_2}{i^2 \eta_F^*} \right] \quad (5)$$

$$K_{J2} \frac{d \ln \bar{N}_2}{dt} = \left[\frac{c_p \eta_T^* \eta_H}{n_{cor,HPT}^2} \left(1 - \frac{1}{e_{HT}}\right) (q_{25} + W_f) - \frac{1}{n_{cor,HPC}^2} \frac{c_p (e_{HC} - 1) q_{25}}{\eta_C^*} \right] \quad (6)$$

Where:

$$K_{J1} = \left(\frac{\pi}{30}\right)^2 J_1, e_{LT} = \pi_{LT}^{\frac{\gamma'-1}{\gamma}}, e_F = \pi_F^{\frac{\gamma-1}{\gamma}}$$

$$K_{J2} = \left(\frac{\pi}{30}\right)^2 J_2, e_{HT} = \pi_{HT}^{\frac{\gamma'-1}{\gamma}}, e_{HC} = \pi_C^{\frac{\gamma-1}{\gamma}}$$

(2) Combustion reaction kinetics modeling

The purpose of fuel combustion modeling is to calculate the outlet temperature T_4 of the combustor (that is, the inlet temperature of the high-pressure turbine), so as to solve the rotor dynamics equation. The reaction rate of the fuel is usually ignored in the differential equation of the combustion chamber, and T_4 is solved by a method of mixing and burning. In this paper, the fuel reaction rate parameter is introduced into the differential equation of the combustion chamber, and the reaction rate is solved by the combustion reaction kinetic equation. The differential equation of the combustion chamber is shown in equation (7).

$$\frac{dT_4}{dt} = \frac{c_{p3}T_3q_3 + \omega_f W_f (h_f + \text{LHV}) - c_{p4}T_4q_4}{\tau c_{p4}q_4} \quad (7)$$

Where T_4 is the exit temperature of the combustion chamber; W_f is the fuel flow rate; LHV is the low fuel heating value; h_f is the fuel enthalpy value; τ is the residence time constant, ω_f is the fuel reaction rate, whose value is determined by the combustion reaction kinetic equation. In this paper, ω_f is added to the differential equation of the combustor to form equation (7), which aims to consider the influence of fuel combustion on temperature when calculating the outlet temperature of the combustor, the main influences include the changing speed of temperature over time, temperature value, and so on.

It can be known from the combustion reaction kinetics that it takes several elementary reactions to decompose the high-carbon mixtures of macromolecules such as aviation kerosene into low-carbon compounds and oxidize low-carbon compounds into products such as carbon dioxide and water. The reaction rate ω_f of aviation kerosene in the multi-step elementary reaction can be obtained by formula (8).

$$\omega_f = \sum_{i=1}^L (v_{fi}'' - v_{fi}') q_i \quad (8)$$

Where L is the number of elementary reactions, and v_{fi}'', v_{fi}' are the equivalent coefficients of reactants and products in the i -th elementary combustion reaction of aviation kerosene. The reaction rate of aviation kerosene in the i -th elementary reaction can be calculated by equation (9).

$$q_i = [k_1 \prod_{j=1}^N (\chi_j)^{v_{ji}'} - k_2 \prod_{j=1}^N (\chi_j)^{v_{ji}''}] \quad (9)$$

Where χ_j represents the molar concentration of aviation kerosene, k_1 , k_2 represent the reaction rate constants of the forward and reverse reactions, which is determined by the Arrhenius formula. The given combustion reaction mechanism is calculated by equation (9) according to the initial conditions of the reaction. Assume Jet A aviation kerosene as the fuel, and select the $C_{12}H_{23}$ mechanism^[11] as the combustion reaction mechanism of Jet A which includes 16 combustion components and 23 elementary reactions, and is given in reference.^[11]

(3) Aero-engine control standard model

Complete aero-engine high-pressure/low-pressure rotor dynamics modeling, combustion reaction dynamics modeling, and merge, simplify, and unify equations in differential forms to form aero-engine control standard model.

Establish aero-engine rotor dynamics equations and combustion chamber differential equations, and introduce combustion reaction kinetic equations into the combustion chamber differential equations to consider the influence of combustion rate on the outlet temperature of the combustion chamber, thus obtaining a aero-engine control standard model, which is shown in equations (10)-(14) as follows. It can be seen from equation (11) that the model adopts the logarithmic form of the high/low pressure rotor speed, which is different from that in the component method, so that the simplest model form can be obtained.

$$\dot{\mathbf{x}} = f(\mathbf{x}) + g(\mathbf{x}) \cdot \mathbf{u} \quad (10)$$

$$\mathbf{x} = [\ln \bar{N}_1 \ln \bar{N}_2 T_4]^T \quad (11)$$

$$\mathbf{u} = [W_f] \quad (12)$$

$$f(\mathbf{x}) = \begin{bmatrix} \frac{1}{K_{J1}} \cdot \left[\frac{c_{p45}}{n_{cor,LPT}^2} \left(1 - \frac{1}{e_{LT}}\right) \eta_T^* q_{25} \eta_L - \frac{1}{n_{cor,FAN}^2 i^2} \frac{c_{p2}(e_F - 1) q_2}{\eta_F^*} \right] \\ \frac{1}{K_{J2}} \cdot \left[\frac{c_{p41}}{n_{cor,HPT}^2} \left(1 - \frac{1}{e_{HT}}\right) \eta_T^* \eta_H - \frac{1}{n_{cor,HPC}^2} \frac{c_{p25}(e_{HC} - 1)}{\eta_C^*} \right] q_{25} \\ \frac{c_{p3} q_3}{\tau c_{p4} q_4} T_3 - \frac{1}{\tau} T_4 \end{bmatrix} \quad (13)$$

$$g(\mathbf{x}) = \begin{bmatrix} \frac{1}{K_{J1}} \cdot \frac{1}{n_{cor,LPT}^2} c_{p45} \left(1 - \frac{1}{e_{LT}}\right) \eta_T^* \eta_L \\ \frac{1}{K_{J2}} \cdot \frac{1}{n_{cor,HPT}^2} c_{p41} \left(1 - \frac{1}{e_{HT}}\right) \eta_T^* \eta_H \\ \frac{(h_f + LHV)}{\tau c_{p4} q_4} \omega_f \end{bmatrix} \quad (14)$$

III. The application of proposed modeling method

The civil aero-engine modeling method oriented to control law design is used in engine modeling, and the model is verified through experiments. Figure 3 is an aero engine experimental platform. The left side of Figure 3 is a small turbofan engine with a large bypass ratio (DGEN380 aero engine), which is used to verify the model. The right side of Figure 3 is the control and monitoring module of the experiment platform.

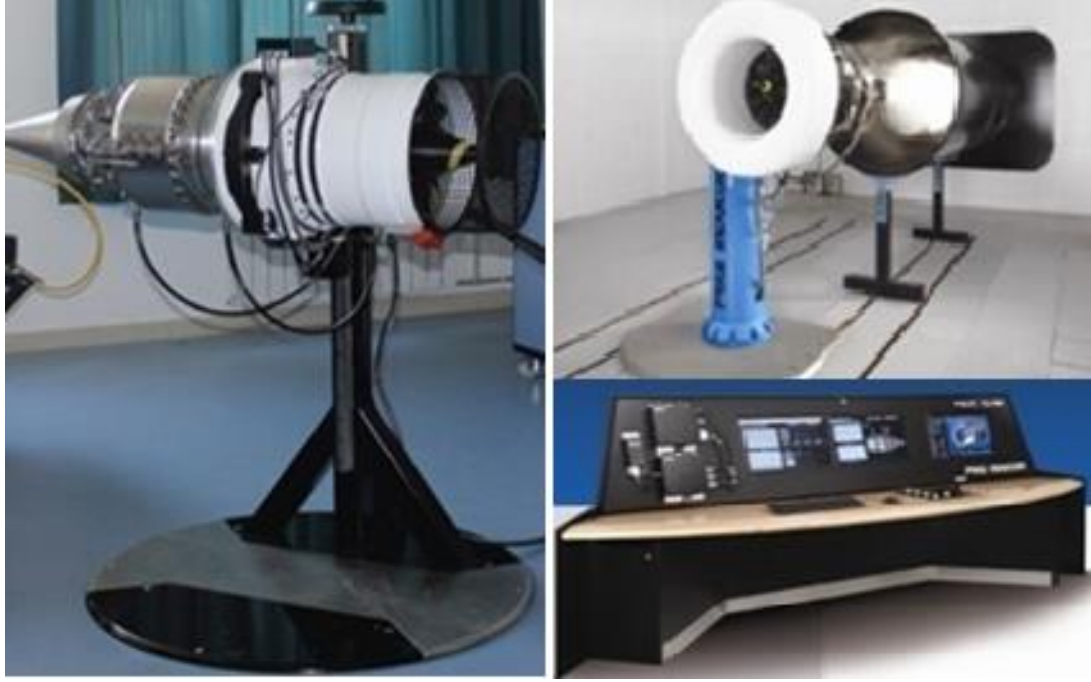


Figure3 Aero-engine test platform

3.1 Civil aero-engine modeling oriented to control law design

(1) Analysis of characteristic parameters of rotating parts

The characteristic parameters of rotating parts include pressure ratio, efficiency, flow rate of fan/compressor and high pressure/low pressure turbine. These characteristic parameters are divided into two parts, one is pressure ratio, and the other part is flow rate and efficiency. The characteristic diagram of aero-engine components show the characteristics of the rotating parts.

For the pressure ratio, the functional relationship between the rotor speed and the pressure ratio can be fitted by the component experimental data^[12], that is, $\pi_i = f(n_i)$. Equations (15) and (16) respectively give the fitting relationship of low-pressure and high-pressure rotors.

$$[\bar{\pi}_F \bar{\pi}_{LT}]^T = \mathbf{A}_1 \cdot [\bar{n}_1^4 \bar{n}_1^3 \bar{n}_1^2 \bar{n}_1]^T + \mathbf{C}_1 \quad (15)$$

$$[\bar{\pi}_C \bar{\pi}_{HT}]^T = \mathbf{A}_2 \cdot [\bar{n}_2^4 \bar{n}_2^3 \bar{n}_2^2 \bar{n}_2]^T + \mathbf{C}_2 \quad (16)$$

$$\mathbf{A}_1 = \begin{bmatrix} 000.4758 & 1.777 \\ 000.19161 & 4.845 \end{bmatrix} \quad \mathbf{C}_1 = \begin{bmatrix} -0.6332 \\ -0.6599 \end{bmatrix}$$

$$\mathbf{A}_2 = \begin{bmatrix} 16.456 & -47.742 & 47.001 & -15.953 \\ 13.217 & -36.695 & 32.974 & -8.2382 \end{bmatrix} \quad \mathbf{C}_2 = \begin{bmatrix} 1.2377 \\ -0.261 \end{bmatrix}$$

(2) Analysis of mechanical efficiency of high-pressure and low-pressure rotors

Consider the change law of the mechanical efficiency of the high-pressure and low-pressure rotors with its speed. The hypothesis of quasi-steady state of the engine state is proposed to calculate the relationship between the mechanical efficiency of the rotor and its rotation speed. The quasi-steady state hypothesis of the engine state is that in a certain steady-state neighborhood of the engine, when the rotation speed changes slightly, the engine power balance equation still holds. The mathematical expression of the quasi-steady state hypothesis of the engine state is as equation (17).

$$\begin{aligned}
&\forall \varepsilon > 0, \\
&\exists |N_s - N| < \varepsilon \\
&\text{s.t. } P_t - P_c = 0
\end{aligned} \tag{17}$$

Where N_s represents the steady state speed. The relationship curve of the mechanical efficiency of the high-pressure/low-pressure rotor with its speed is obtained according to the quasi-steady state assumption of the engine state.

Figure 4 shows the efficiency curve of the DGEN380 aero-engine, in which the abscissa represents the relative value of the rotor speed, and the ordinate represents the mechanical efficiency of the rotor. The trend of mechanical efficiency and speed of the two rotors are similar. When the rotation speed is low (the relative value of the rotation speed is less than 0.6), as the rotation speed increases, the mechanical efficiency has a tendency to first decrease and then rise; when the rotation speed is high, the mechanical efficiency increases with the increase in the rotation speed.

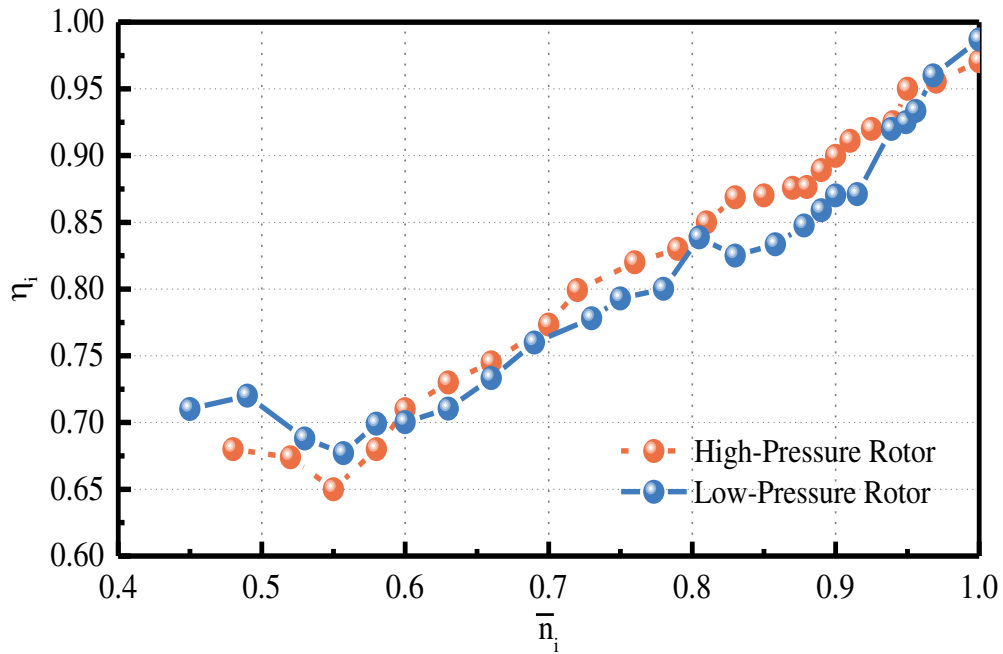


Figure4 The relationship curve of the mechanical efficiency of the rotor with the relative value of the speed

3.2 Aero-Engine Control Standard Model of DGEN380

The parameter values are determined through the characteristic parameter analysis of the rotating parts and the mechanical efficiency analysis of the high/low pressure rotor. Finally formulas (10)-(14) are obtained, and a model that can be directly used for the design of control laws is obtained. The model involves rotor dynamics equations and combustion reaction dynamics equations, and the time scale of rotor rotation (10^{-1} s) and the time scale of combustion reaction (10^{-3} s- 10^{-5} s) are set quite different to consider the differential equations rigidity when solving the model.

The ODE15s solver with variable order and multi-step solving is selected to solve the DGEN380 aero-engine control standard model.

(1) Analysis of steady-state calculation results of model

The control standard model of DGEN380 aero-engine is solved according to the altitude, Mach number, and fuel flow value corresponding to each state point of the engine given in the manual of DGEN380 aero-engine. The state of aero-engine includes idle state (PLA=0°), cruise state (PLA=43°) and climb state (PLA=74°).

Enter the initial condition of equation (10), that is $[\bar{N}_1^0 \bar{N}_2^0 \bar{T}_4^0]$, and perform a steady-state solution. The steady-state solution results are shown in Table 1. The relative error of the model solution value is calculated based on the values given in the manual, as shown in Table 1. The maximum error of the steady-state calculation of model is 0.43%. This value indicates that the established DGEN380 aero-engine control standard model can accurately reflect the steady state of the DGEN380 aero-engine.

Table1 Steady-state solution results of control standard MS model of DGEN380

	N ₁ relative value			N ₂ relative value			T ₄ relative value		
	Manual	Simulate	Error	Manual	Simulate	Error	Manual	Simulate	Error
	Value	Result	(%)	Value	Result	(%)	Value	Result	(%)
Idle	0.4701	0.47006	0.009	0.5676	0.56761	0.002	0.6516	0.65154	0.009
Cruise	0.925	0.9251	0.011	0.9559	0.95594	0.004	0.939	0.93902	0.002
Climb	1	1.00043	0.043	1	1.00026	0.026	1	1.00034	0.034

(2) Analysis of model transition state calculation results

The transition state is solved on the basis of the steady-state solution, and the transition curve between each steady-state point of the engine state parameters is obtained. Figure 5 shows the aero-engine power spectrum, in which the abscissa represents time, and the ordinate is the angle of the throttle lever to represent the power state of the aero-engine. At the 10th second, the throttle lever is quickly pushed from 0° to 74°, which makes the engine state transition from the idle state to the climb state; at the 30th second, the throttle lever is retracted to 0°, and the engine state returned to the idle state; at the 77th second, The throttle lever is quickly pushed from 0° to 74°, so that the engine state transitions from the idle state to the climb state; at the 151st second, the throttle lever angle is quickly retracted from 74° to 43°, and the engine state transitions from the climb state to the cruise state; At the 190th second, the throttle lever quickly returned to 0°, and the engine state returned to the idle state. Figure 6 shows the fuel supply curve corresponding to the engine power spectrum, which shows the relationship between the fuel flow rate and time. During the experimental, H=0m, adjust the airflow parameters of the aero engine so that the airflow speed Ma=0.338, to ensure that the flight conditions of the model are consistent with the experimental conditions. Take the parameter value $[N_1 \bar{N}_2 \bar{T}_4]$ of the idle state as the initial value of the differential equation, and then obtain the calculation results of the transition state of the DGEN380 aero-engine control standard mode, which are shown in Figure 7-9.

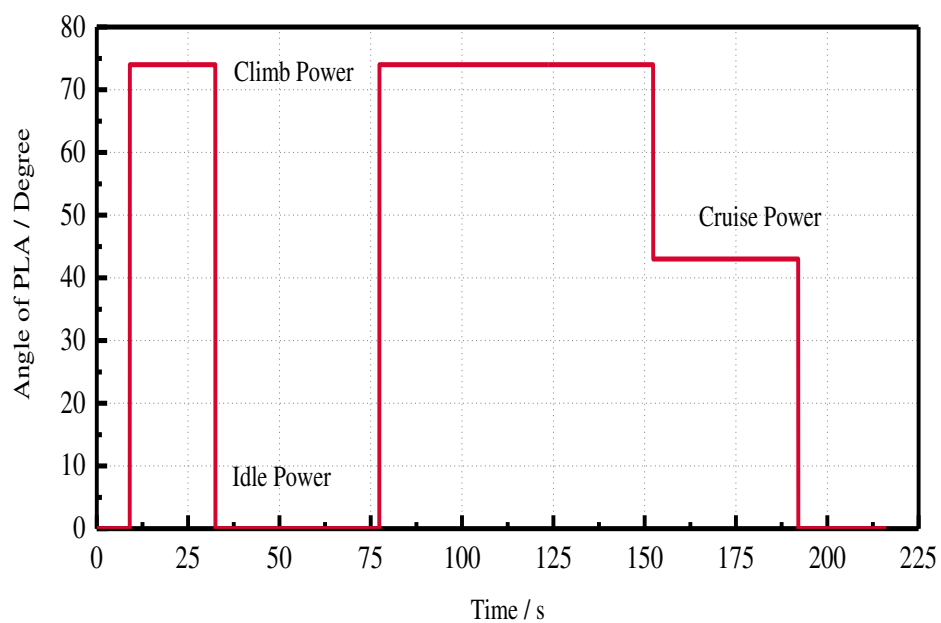


Figure5 Power spectrum diagram of DGEN380

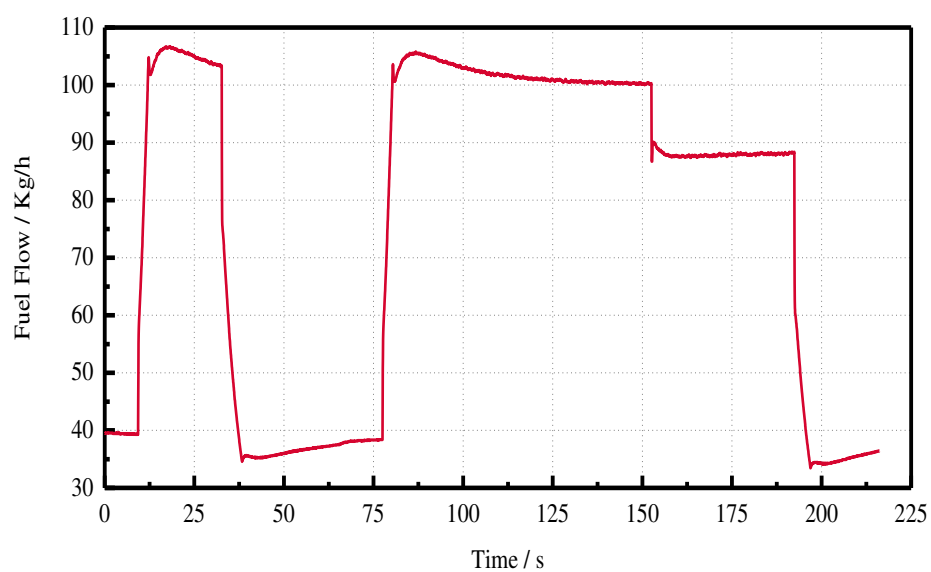


Figure6 Fuel supply curve of DGEN380 aero-engine

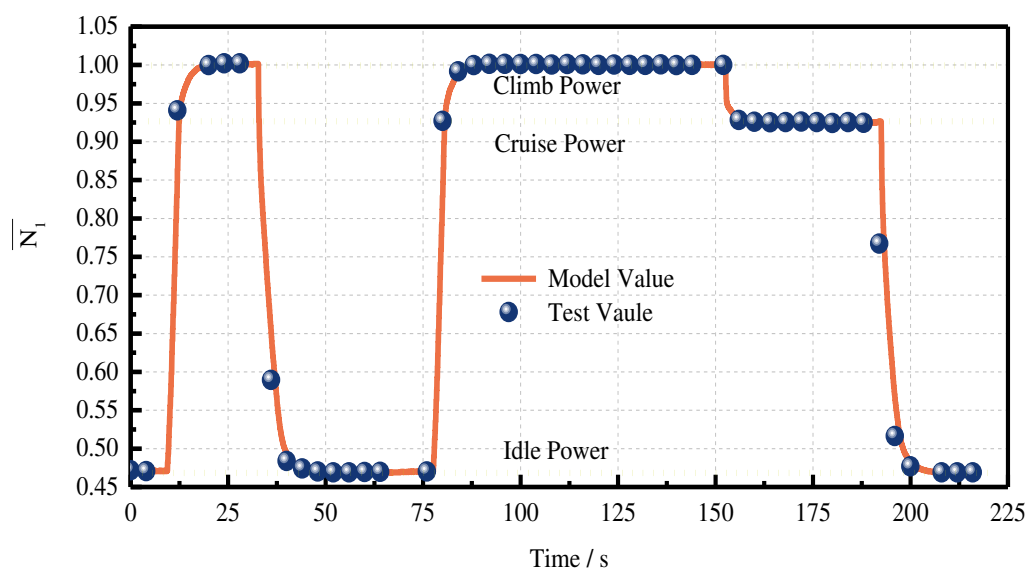


Figure7 Open loop response curve of relative value of low pressure rotor speed

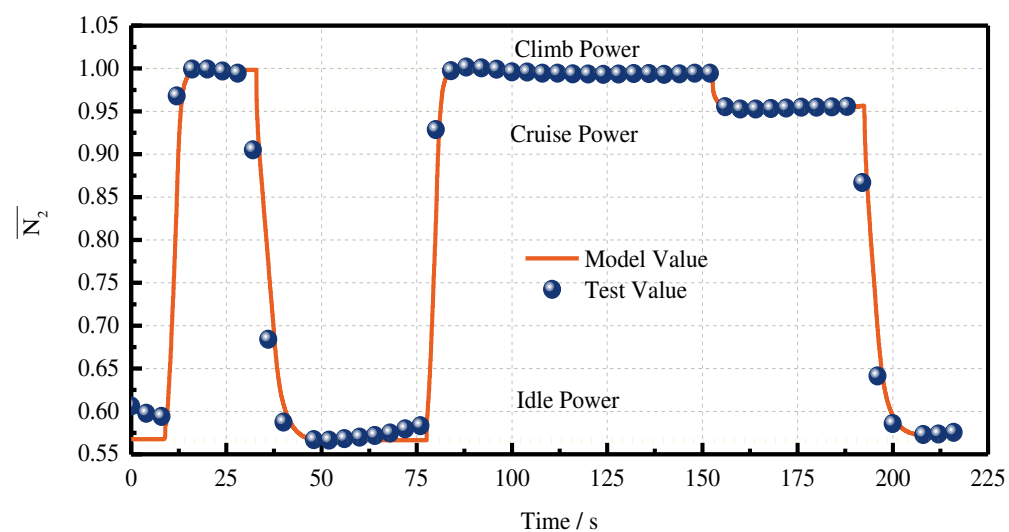


Figure8 Open-loop response curve of relative value of high-pressure rotor speed

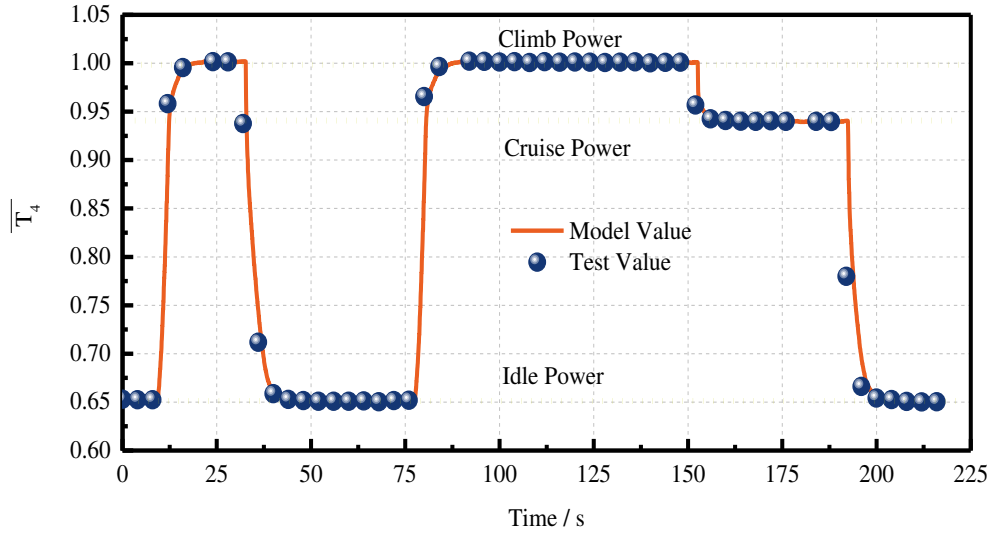


Figure9 Open-loop response curve of the relative value of the outlet temperature of the combustion chamber

2.3 The example of control law design based on control standard model

Taking the sliding mode variable structure control method as an example, design the non-linear control law of aero-engine according to the aero-engine control standard model to realize the thrust control function.

The low-pressure rotor speed N_1 and the combustion chamber outlet temperature T_4 are used as the control parameters, and the vector y is set as in equation (18). The control goal is to make the vector y equal to the zero.

$$y = \begin{bmatrix} y_1 \\ y_2 \end{bmatrix} = \begin{bmatrix} N_1 - N_{1,ref} \\ T_4 - T_{4,ref} \end{bmatrix} \quad (18)$$

The parameter index ref in the formula represents the command value. The correlation between the input vector of the control standard MS model and the vector y is $[1 \ 1]$. According to the definition of vector y , suppose the correlation degree of each sliding function in the sliding mode vector is 1, then the sliding mode vector is set as equation (19)

$$S = \begin{bmatrix} S_1 \\ S_2 \end{bmatrix} = \begin{bmatrix} y_1 \\ y_2 \end{bmatrix} \quad (19)$$

The form of the control standard MS model is the normative form to describe the dynamic system. According to the control standard MS model, the sliding mode vector S has the form of equation (20).

$$\dot{S} = \varphi_1(\bullet) + \varphi_2(\bullet) \bar{u} \quad (20)$$

Where function vector $\varphi_1(\bullet)$ and $\varphi_2(\bullet)$ are as follows:

$$\varphi_1(\bullet) = \begin{bmatrix} \frac{1}{K_{J1}} \cdot \frac{1}{n_{cor,LPT}^2} \cdot (W_{LPT} \cdot q_{m,LPT} \cdot \eta_{lm} - W_{Fan} \cdot q_{m,Fan}) \\ \frac{R \cdot T_4 \cdot q_{m,in}}{C_V \cdot P_4 \cdot V} \cdot (C_p - C_V) \cdot (T_3 - T_4) \end{bmatrix} \quad (21)$$

$$\boldsymbol{\varphi}_2(\bullet) = \begin{bmatrix} \frac{1}{K_{Jl}} \cdot \frac{1}{n_{cor,LPT}^2} \cdot W_{LPT} \cdot \eta_{lm} \\ \frac{R \cdot T_4}{C_V \cdot P_4 \cdot V} \cdot (C_V - C_p) \cdot T_4 \end{bmatrix} \quad (22)$$

Considering the influence of uncertainty, the function vectors $\boldsymbol{\varphi}_1(\cdot)$ and $\boldsymbol{\varphi}_2(\cdot)$ are written as the sum of the nominal value and the uncertain value, as shown in equations (23) and (24).

$$\boldsymbol{\varphi}_1 = \boldsymbol{\varphi}_{1N} + \Delta\boldsymbol{\varphi}_1 \quad (23)$$

$$\boldsymbol{\varphi}_2 = \boldsymbol{\varphi}_{2N} + \Delta\boldsymbol{\varphi}_2 \quad (24)$$

Where $\boldsymbol{\varphi}_{1N}$ 、 $\boldsymbol{\varphi}_{2N}$ represent nominal value, and $\Delta\boldsymbol{\varphi}_1$ 、 $\Delta\boldsymbol{\varphi}_2$ represent uncertain value. Suppose for $\mathbf{x} \in \mathbf{X}$, $t \geq 0$, then $\Delta\boldsymbol{\varphi}_1(\mathbf{x}, t)$ 、 $\Delta\boldsymbol{\varphi}_2(\mathbf{x}, t)$ satisfy formula (25):

$$\left| \frac{\Delta\varphi_i}{\varphi_i} \right| < 1, (i = 1, 2) \quad (25)$$

Set the control law as equation (26).

$$\dot{\mathbf{S}} = (\Delta\boldsymbol{\varphi}_1 - \boldsymbol{\varphi}_{2N}^{-1} \boldsymbol{\varphi}_{1N} \Delta\boldsymbol{\varphi}_2) + (\mathbf{I}_{2 \times 2} + \boldsymbol{\varphi}_{2N}^{-1} \Delta\boldsymbol{\varphi}_2) \boldsymbol{\theta} \quad (26)$$

Set $\mathbf{S}_A = \Delta\boldsymbol{\varphi}_1 - \boldsymbol{\varphi}_{2N}^{-1} \boldsymbol{\varphi}_{1N} \Delta\boldsymbol{\varphi}_2$, $\mathbf{S}_B = \mathbf{I}_{2 \times 2} + \boldsymbol{\varphi}_{2N}^{-1} \Delta\boldsymbol{\varphi}_2$. It can be seen from equation 2.43 that \mathbf{S}_A and \mathbf{S}_B are bounded, so equation (27) holds.

$$\begin{aligned} \forall \mathbf{x} \in \mathbf{X}, t \geq 0 \\ |\mathbf{S}_A| \leq \mathbf{S}_{AM} \\ 0 < \mathbf{S}_{Bm} \leq |\mathbf{S}_B| \leq \mathbf{S}_{BM} \end{aligned} \quad (27)$$

The control goal is to make the sliding mode vector \mathbf{S} tend to $\mathbf{0}$ within a finite time. When \mathbf{S}_A and \mathbf{S}_B are uncertain and unknown, the control input vector $\boldsymbol{\theta}$ in the sliding mode is shown in equation (28).

$$\boldsymbol{\theta} = \begin{bmatrix} K_1 \text{sign}(S_1) \\ K_2 \text{sign}(S_2) \end{bmatrix} \quad (28)$$

Where K_1 and K_2 are the gain coefficients of the sliding mode control law, whose values satisfy formula (29), and λ is positive.

$$K > \frac{S_{AM} + \lambda}{S_{Bm}} \quad (29)$$

The sliding mode control law can satisfy the sliding mode condition $\dot{\mathbf{S}} \leq \lambda |\mathbf{S}|$ ($\dot{\mathbf{S}} < 0$) to ensure that the sliding mode vector \mathbf{S} tends to $\mathbf{0}$ within a finite time. Choose $\lambda=0.001$ to simulate the sliding mode control law according to formula (29). White noises with amplitudes of 0.005^2 and 0.004^2 are added to the low-pressure rotor speed and the outlet temperature of the combustion chamber respectively during the simulation experiment, The simulation time is 6s. At 0s, the aero-engine is stable in the idle state, and at 1s, the throttle lever is quickly pushed from 0° to 74° . Figure 10 and Figure 11 show the simulation results of the sliding mode control law.

So the design of the aero-engine nonlinear control law is completed. The control standard model has a simple form and a standardized format, which can be directly used in the design of a sliding mode variable structure controller. Under the action of the control input vector, the thrust control of the aero-engine can be realized.

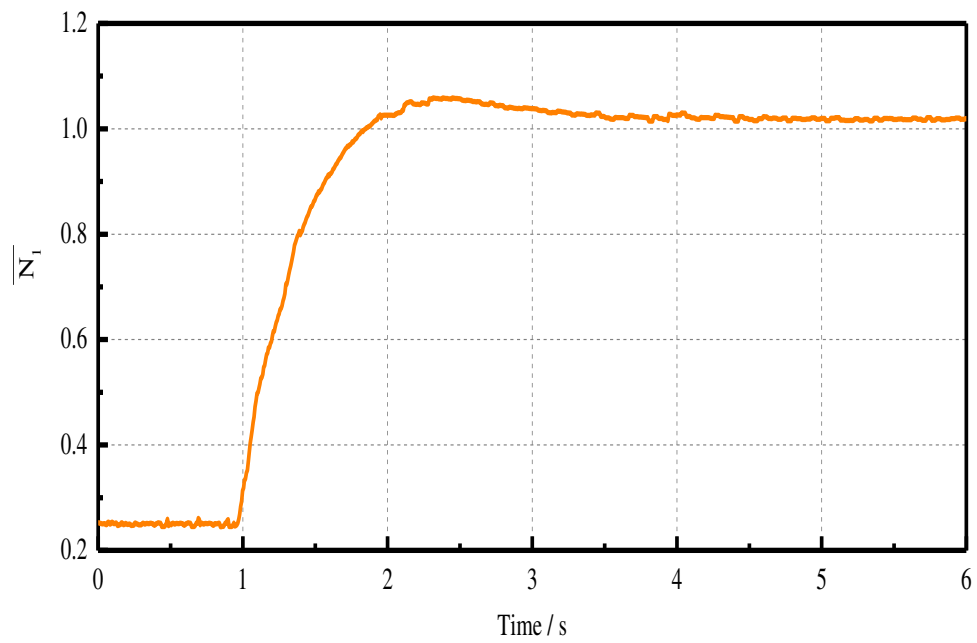


Figure10 The response curve of the relative value of the low pressure rotor speed

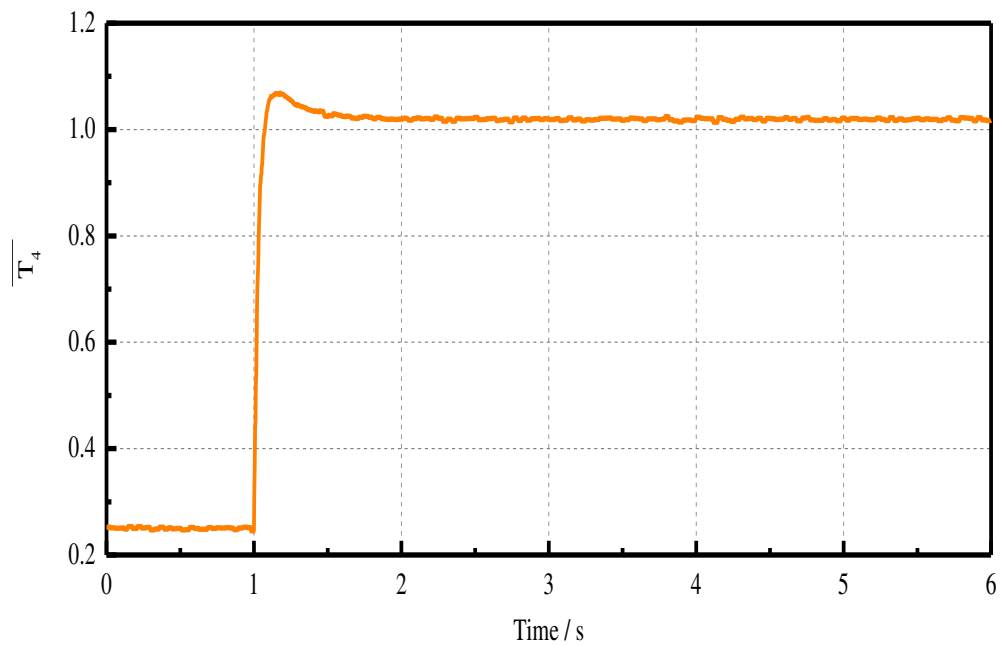


Figure11 The response curve of the relative value of the outlet temperature of the combustion chamber

4.Conclusion

A civil aviation engine modeling method oriented to control law design is

proposed in this paper. Simplify model structure according to aero-engine control function, and establish aero-engine control standard model in the differential form through rotor dynamics modeling and combustion reaction dynamics modeling. The control standard model directly used in the design of the controller has a small amount of calculation. The model establishes the corresponding relationship between the parameters required for the control in the full envelope of the aero-engine, and the nonlinear control method can be directly used in the design of the aero-engine control law, which simplifies the workload and difficulty of control law design to a certain extent.

The civil aero-engine modeling method oriented to control law design establishes the aero-engine control standard model of DGEN380. The maximum error of the model is 0.43% in the steady state, the maximum relative deviation of the model state parameters in transition state is 0.3516%, and the maximum lag time is 0.08333 seconds. Design successfully a nonlinear control law on the basis of the control standard model by taking the sliding mode method as an example. The control standard model used in the design of aero-engine control law can simplify the design process, reduce the workload, and reduce the design difficulty.

references

- [1] Hanz Richter. Advanced Control of Turbofan Engines. Cleveland State University. Springer,2012
- [2] Eberle C, Gerlinger P, Geigle K P, et al. Numerical investigation of transient soot evolution processes in an aero-engine model combustor[J]. Combustion Science and Technology, 2015, 187(12): 1841-1866.
- [3] Bai Jie, Liu Shuai,Wang Wei.Identification method for parameter uncertain model of aero-engine. [J]. Journal of Aerospace Power,2020,35(01):178-184.
- [4] Zheng Q, Fang J, Hu Z, et al. Aero-engine on-board model based on batch normalize deep neural network[J]. IEEE Access, 2019, 7: 54855-54862.
- [5] Otto E W, Taylor B L. Dynamics of a Turbojet Engine Considered as a Quasi Static System[R].NACA TN-2091.1950
- [6] Seldner K. Generalized simulation technique for turbojet engine system analysis[M]. New York: National Aeronautics and Space Administration, 1972.
- [7] Szuch R. HYDES: a generalized hybrid computer program for studying turbojet or turbofan engine dynamics[R]. Ohio: NASA/TM, 1974.
- [8] Sellers F, Daniele J. DYNGEN: A program for calculating steady-state and transient performance of turbojet and turbofan engines[M]. New York: National Aeronautics and Space Administration, 1975.
- [9] Turner G, Reed A, Ryder R, et al. Multi-fidelity simulation of a turbofan engine with results zoomed into mini-maps for a zero-d cycle simulation[C]//ASME Turbo Expo 2004: Power for Land, Sea, and Air. American Society of Mechanical Engineers Digital Collection, 2004: 219-230.
- [10] Wen X, Luo Y, Luo K, et al. LES of pulverized coal combustion with a multi-regime flamelet model[J]. Fuel, 2017, 188: 661-671.
- [11] Kundu K, Penko P, Yang S. Reduced reaction mechanisms for numerical calculations in combustion of hydrocarbon fuels[C]//36th AIAA Aerospace Sciences Meeting and Exhibit. 1998: 803.
- [12] Qian F,Abaid N, Zuo L. Multiple-Scale Analysis of a Tunable Bi-Stable Piezoelectric

- Energy Harvester[J]. ASME. Letters Dyn. Sys. Control. 2021; 1(2): 021006.
- [13] Bhattacharya C, Ray A. Data-Driven Detection and Classification of Regimes in Chaotic Systems Via Hidden Markov Modeling[J]. ASME. Letters Dyn. Sys. Control 2021; 1(2): 021009.